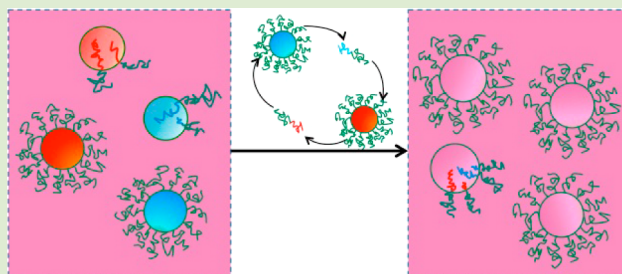


# Molecular Exchange in Diblock Copolymer Micelles: Bimodal Distribution in Core-Block Molecular Weights

J. Lu,<sup>†</sup> S. Choi,<sup>†</sup> F. S. Bates,<sup>\*,†</sup> and T. P. Lodge<sup>\*,†,‡</sup>

<sup>†</sup>Departments of Chemical Engineering and Materials Science and <sup>‡</sup>Chemistry, University of Minnesota, Minneapolis, Minnesota 55455, United States

**ABSTRACT:** The role of core block size dispersity on the rate of molecular exchange in spherical micelles formed from 1% by volume poly(styrene-*b*-ethylene-propylene) (PS-PEP) diblock copolymers in squalane (C<sub>30</sub>H<sub>62</sub>) was investigated using time-resolved small-angle neutron scattering (TR-SANS). Separate copolymer solutions (total polymer 1% by volume) containing either deuterium labeled (dPS) or normal (hPS) poly(styrene) core blocks were prepared and mixed at room temperature, below the core glass transition temperature. Each preparation (dPS or hPS) contained equal volume fractions of  $M_n = 26$  and 42 kg/mol (h-equivalent) poly(styrene) blocks. Heating to temperatures between 87 and 146 °C resulted in block copolymer exchange as evidenced by a systematic reduction in the SANS intensity; C<sub>30</sub>H<sub>62</sub> and C<sub>30</sub>D<sub>62</sub> were blended so as to contrast match the fully exchanged cores. Following a protocol established in a previous report, the time-dependent intensity data were shifted with respect to time and temperature, leading to a master curve covering nearly 7 orders of magnitude in reduced time. These results are quantitatively accounted for by summing the weighted relaxation functions obtained from the individual components, consistent with a previously published model that accounts for the dramatic sensitivity of the molecular exchange dynamics to core block dispersity.



Amphiphilic block polymers offer a variety of advantages in the design and application of self-assembled micelles across a host of technologies, including drug delivery,<sup>1,2</sup> toughening of plastics,<sup>3,4</sup> and viscosity modification for use in enhanced oil recovery and motor lubricants.<sup>5–7</sup> While the molecular factors responsible for controlling micelle aggregation number and structure (e.g., spheres, cylinders, and vesicles) are similar to those governing low molecular weight surfactants,<sup>8–10</sup> a macromolecular architecture leads to qualitatively different micelle dynamics.<sup>11</sup> In 2001, Willner et al.<sup>12</sup> first reported kinetically frozen poly(ethylene-propylene-*b*-ethylene oxide) (PEP-PEO) micelles in aqueous solution, where no chain exchange was observed by time-resolved small-angle neutron scattering (TR-SANS). Later, poly(butadiene-*b*-ethylene oxide) (PB-PEO) micelles were shown by TR-SANS<sup>13</sup> and cryogenic transmission electron microscopy (cryoTEM)<sup>14</sup> to be nonergodic when dispersed in water at molecular weights as low as 3000 g/mol. Similar polymers were also shown by TR-SANS to undergo no exchange in ionic liquids, even at temperatures as high as 200 °C.<sup>15</sup> Pioneering experiments by Lund et al. based on TR-SANS with PEP-PEO diblock oligomers in water/*N,N*-dimethylformamide (DMF) mixtures<sup>16,17</sup> and poly(styrene-*b*-butadiene) diblock copolymers, as well as poly(styrene-*b*-butadiene-*b*-styrene) triblock copolymers, in various *n*-alkane solvents<sup>18,19</sup> have shown that the associated dynamics of molecular exchange are logarithmically dependent on time as opposed to the intuitive exponential form.<sup>20</sup> TR-SANS measurements with relatively high molecular weight poly(styrene-*b*-ethylene-propylene) (PS-PEP) diblock

copolymers dissolved in squalane (C<sub>30</sub>H<sub>62</sub>) revealed that the origins of this behavior can be traced to a finite distribution in core (PS) block molecular weight.<sup>21</sup> Remarkably, even a relatively small spread in the distribution of PS core block sizes ( $\mathcal{D} = M_w/M_n < 1.1$ ) was shown to produce dramatic broadening of the rate of molecular exchange, both in disordered (1% by volume block copolymer)<sup>21</sup> and ordered (15%)<sup>22</sup> spherical micelles. In a recent publication, Zinn and co-workers<sup>23</sup> have shown that molecular exchange in aqueous solutions of *n*-alkyl-PEO diblocks ( $n = 18, 24,$  and 30) containing strictly monodisperse ( $\mathcal{D} = 1$ ) core blocks is exponential in time, consistent with the theoretical model proposed by Choi et al.<sup>21</sup> This model is an extension of the detailed model of Halperin and Alexander<sup>20</sup> but explicitly considers the dispersity of the core block and proposes an alternate dependence of the activation barrier on the core block length (proportional to  $N_{\text{core}}$  rather than  $N_{\text{core}}^{2/3}$ ).

This letter reports a new TR-SANS study that quantitatively confirms the predicted form of the molecular exchange dynamics in spherical micelles prepared with an intentionally broadened distribution in core block molecular weights. We have blended pairs of relatively monodisperse PS-PEP diblocks, where the PS block molecular weights differ by a factor of 1.6. Normal (hPS-PEP-1 and hPS-PEP-2) and selectively deuterated (dPS-PEP-1 and dPS-PEP-2) diblocks were synthesized by

Received: June 7, 2012

Accepted: July 9, 2012

Published: July 19, 2012

sequential anionic polymerization of styrene and isoprene, followed by homogeneous catalytic saturation of the poly-(isoprene) blocks with deuterium, as described previously<sup>24</sup> (see Table 1). The molecular weight distribution of the

**Table 1. Diblock Copolymer Characteristics<sup>a</sup>**

polymer	$N_{PS}^b$	$N_{PEP}^c$	$\mathcal{D}$
hPS-PEP-1	250	970	1.04
dPS-PEP-1	260	985	1.10
hPS-PEP-2	400	880	1.05
dPS-PEP-2	423	926	1.10

<sup>a</sup>Adapted from ref 21. <sup>b</sup>Number of PS repeat units. <sup>c</sup>Number of PEP repeat units.

individual diblocks is relatively narrow ( $\mathcal{D} \leq 1.1$ ) and the average degree of polymerization of the PS blocks falls into two categories:  $\langle N_{PS} \rangle \cong 255$  and 412.

Figure 1 illustrates the contrast matching strategy underlying the TR-SANS experiment. A solution containing equal volume

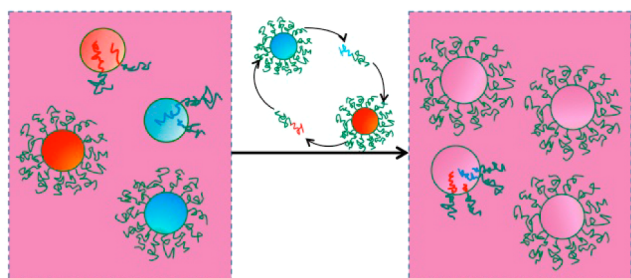


**Figure 1.** Chain exchange in a postmixed sample of spherical micelles formed by mixing pairs of hPS-PEP (blue PS cores) and dPS-PEP (red PS cores), containing two different molecular weight PS blocks. Complete chain exchange results in a uniform distribution of the four types of PS blocks, which contrast matches the isotopically labeled squalane solvent.

fractions of micelles with protonated (hPS) and deuterated (dPS) cores (referred to as a “post-mixed” specimen, see below) is rapidly heated to a target temperature and a series of SANS patterns are recorded over time under isothermal conditions. The isotopic composition of the solvent is chosen so as to match the neutron scattering length density ( $\rho$ ) of the micelle cores after complete molecular exchange,  $\rho_{\text{solvent}} = (\rho_{\text{d,core}} + \rho_{\text{h,core}})/2$ . Because the intensity of neutrons scattered by a micelle core is proportional to the contrast factor,  $I \sim (\rho_{\text{solvent}} - \rho_{\text{core}})^2$ , the SANS intensity associated with the micelle scattering affords direct access to the extent of molecular exchange.

Micelle solutions containing 1% by volume diblock copolymer were prepared using the cosolvent method. Polymers were dissolved in squalane and excess dichloromethane (a neutral cosolvent that dissolves both blocks at room temperature), and the dichloromethane was removed by evaporation, leading to the formation of spherical micelles. Subsequently, the micelle solutions were annealed at 190 °C for 30 min to allow complete equilibration.<sup>24</sup> Two types of solutions were prepared for SANS analysis: “pre-mixed” and “post-mixed.” Premixed specimens were formed by mixing all four polymers in squalane and dichloromethane followed by evaporation of the volatile component and annealing, resulting in a solution of micelles containing equal volume fractions of

both dPS and both hPS blocks. The isotopic composition of the squalane (42 vol %  $C_{30}H_{62}$  and 58 vol %  $C_{30}D_{62}$ ; Sigma-Aldrich and C/D/N Isotopes, respectively) was selected to contrast match the preformed micelle cores. Preparation of the (1% by volume polymer) postmixed solutions began with the formation of two isotopically pure mixtures, one with hPS-PEP-1 and hPS-PEP-2 (50% by volume of each hPS block type) and a second with dPS-PEP-1 and dPS-PEP-2 (also with equal volume fractions of each dPS block type). Equal portions of these isotopically pure solutions were then combined at room temperature. Because the PS cores are glassy at room temperature, no molecular exchange occurs with the postmixed specimens until they are heated above the core (PS) glass transition temperature,  $T_{g,PS} \cong 70$  °C.<sup>25</sup>

TR-SANS experiments were performed with the CG-2 General-Purpose SANS instrument at the High Flux Isotope Reactor (HFIR) facility of Oak Ridge National Laboratory (ORNL) using a sample-to-detector distance of 14 m and neutrons with wavelength  $\lambda = 4.75$  Å. Data reduction was performed using the Igor package provided by ORNL. Polymer solutions (1 vol %) were loaded into quartz cells (1 mm sample thickness) and inserted into a preheated and temperature controlled ( $\pm 0.2$  °C) copper block fitted with two quartz windows for thermal stability. The actual temperature was calibrated using a thermocouple immersed in oil in a separate quartz cell. About 5 min was required for a specimen to stabilize within 1 °C of the set temperature, at which point SANS data acquisition was initiated; 2-D scattering patterns were recorded in 5 min increments for up to 3 h. Representative TR-SANS results, obtained at 108 °C, are shown in Figure 2.

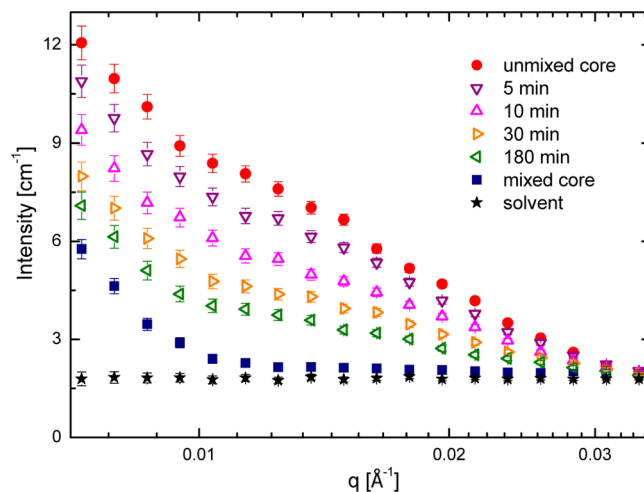


**Figure 2.** Representative TR-SANS patterns recorded in 5 min increments during molecular exchange of PS-PEP in squalane at 108 °C.

Changes in the SANS intensity were monitored as a function of time at constant temperature over the range  $0.01 \leq q \leq 0.04$  Å<sup>-1</sup>, where  $q = 4\pi\lambda^{-1}\sin(\theta/2)$ . Figure 2 illustrates a representative set of results. Relative changes in the concentration of dPS blocks in the micelles can be related to a dimensionless molecular relaxation function,<sup>16</sup>

$$R(t) = \left[ \frac{I(t) - I(\infty)}{I(0) - I(\infty)} \right]^{1/2} \quad (1)$$

where  $I(0)$  and  $I(t)$  represent the (integrated) initial scattered intensity and that recorded at elapsed time  $t$  and  $I(\infty)$  is the scattering intensity at infinite time;  $I(\infty)$  can be closely approximated using the premixed specimen.

Relaxation functions, acquired at seven different temperatures, are presented in Figure 3. At the lowest measurement

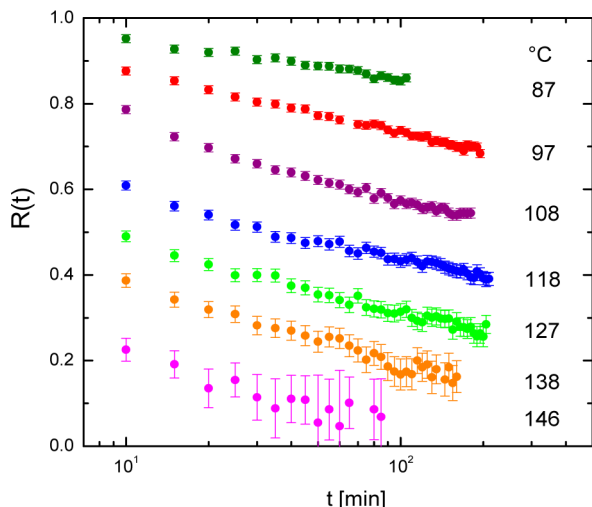


**Figure 3.**  $R(t,T)$  determined by TR-SANS for postmixed solutions of binary dPS-PEP and hPS-PEP mixtures. The spherical micelle cores were formed with equal amounts by volume of two PS blocks that differ by 60% in degree of polymerization.

temperature, 87 °C, approximately 15% of the initial intensity recorded for the postmixed sample is lost over 100 min of time. At the highest temperature, 146 °C,  $R(t)$  dropped by more than 90% over a comparable period. TR-SANS experiments conducted at all seven temperatures provided access to a wide range of molecular exchange,  $0.1 \leq R(t,T) \leq 0.95$ , as shown in Figure 3.

In an earlier publication that dealt with molecular exchange between equal molecular weight diblock copolymers (dPS-PEP-1/hPS-PEP-1 and dPS-PEP-2/hPS-PEP-2) we demonstrated that master curves could be constructed from  $R(t,T)$  data using the time–temperature superposition principle,<sup>26</sup> that is,  $R(t/a_T, T_{\text{ref}}) = R(t,T)$ , where  $a_T$  and  $T_{\text{ref}}$  are the shift factor and reference temperature, respectively.<sup>21</sup> Figure 4a illustrates application of this technique to the results shown in Figure 3; the corresponding  $\log[a_T(T)]$  is plotted versus  $T$  in Figure 4b. Significantly, within experimental uncertainty the  $a_T$  values determined with the binary blends match those associated with the individual components, consistent with the assumption that the temperature dependence of the exchange dynamics is controlled primarily by polystyrene segmental motion, that is, free volume.

Choi et al.<sup>21</sup> modeled the molecular exchange dynamics of the monomodal diblock copolymer based micelles subject to the following assumptions: (i) single chain expulsion/insertion is the dominant mechanism; (ii) extraction of a core block is the rate limiting step; (iii) motions of the unentangled core blocks are governed by Rouse dynamics; (iv) the energy barrier  $E_a$  for ejecting a block copolymer into the solvent/corona matrix is proportional to the core block length. A first-order relaxation function for the extraction of an individual core block with degree of polymerization  $N_i$  subject to Rouse dynamics with a longest relaxation time  $\tau_{\text{Rouse}}$  yields  $K(t, N_i) = \exp(-t$

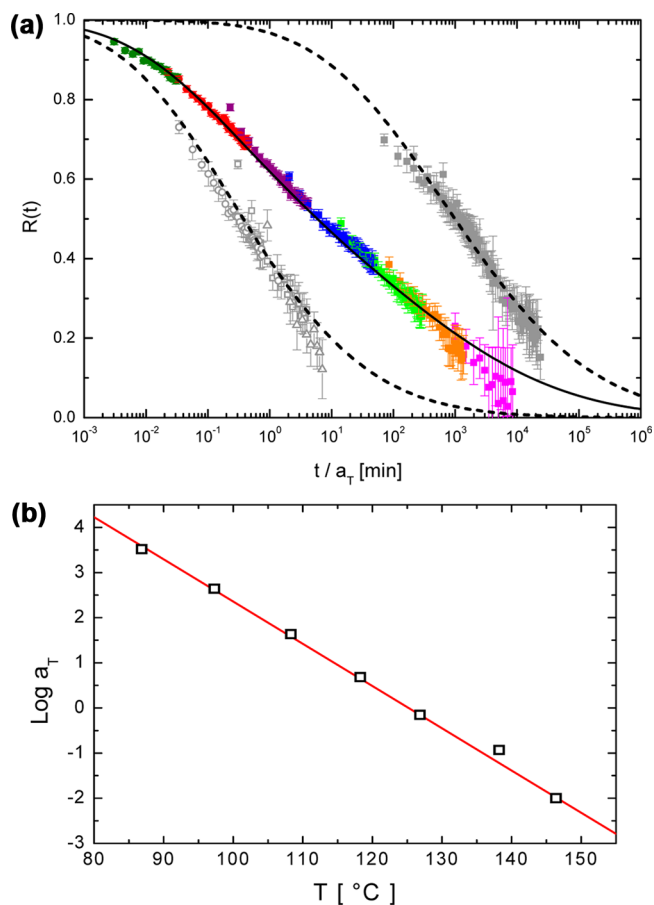


**Figure 4.** (a) Master curve for the TR-SANS results shown in Figure 3 following time–temperature superposition with  $T_{\text{ref}} = 125$  °C. Colored symbols identify the measurement temperatures as shown in Figure 3. Gray symbols and dashed curves represent the master curves and model fits, respectively, reported earlier for the individual low and high molecular weight PS-PEP constituents used in the blended specimens.<sup>21</sup> The solid curve is calculated using eq 2 and the two dashed curves without any adjustable parameters. (b) Time–temperature shift factors (open symbols) extracted from the time–temperature shifted data for the binary blends in (a). The solid curve represents  $a_T(T)$  reported earlier for the individual (monomodal) components.<sup>21</sup>

$/\tau(N_i))$ , where  $\tau(N_i) = \tau_{\text{Rouse}}(N_i) \times \exp(E_a(N_i)/kT)$ . In order to account for a distribution of chain lengths  $K(t, N_i)$  is multiplied by a Zimm-Schulz distribution function  $P(N_i)$  and the product is integrated over all  $N_i$  yielding  $R(t)$ . Only two parameters were adjusted in arriving at the model fits shown by the dashed curves in Figure 4a: the core block dispersity ( $\mathcal{D}$ ) and the combination parameter  $\alpha\chi$ , which accounts for the enthalpic penalty of exposing core segments to the solvent/corona matrix, where  $\chi$  is the Flory–Huggins parameter and  $\alpha$  is an  $O(1)$  constant.<sup>27–29</sup> The values of  $\mathcal{D}$  were 1.08 and 1.04 for PS-PEP-1 and PS-PEP-2, respectively. The values of  $\alpha\chi$  were 0.041 and 0.042 for the two polymers, which compare favorably with the reported value of  $\chi$  for PS-PEP of 0.07.<sup>30</sup>

This model assumes that the overall rate of molecular exchange represents the sum of individual core block expulsion events. Hence,  $R(t)$  for a binary mixture of two monomodal populations of core blocks should be represented by the weighted sum of the component relaxation functions,

$$R(t)_{\text{binary mixture}} = \nu_1 R_1(t) + (1 - \nu_1) R_2(t) \quad (2)$$

where  $\nu_1$  and  $R_1(t)$  are the mole fraction and relaxation function, respectively, for species 1. We have calculated the model prediction for the blend master curve (solid curve in Figure 4a) based on the previous model results for PS-PEP-1 and PS-PEP-2 (dashed curves in Figure 4a) with  $\nu_1 = 0.61$  (see Table 1). Here we emphasize that this result, which accounts for the experimental data over nearly 7 orders of magnitude in reduced time, was obtained without any adjustable parameters. Swelling of micelle cores would lead to faster kinetics. We have reported previously that the swelling of PS cores in squalane is negligible below 100 °C but increases thereafter.<sup>24</sup> Based on our previous results, the solvent fraction in core is about 10% at 138 °C. Consequently, one might expect an acceleration in exchange rate with increasing temperature due to swelling, but it would likely not be evident in the empirical shift factors themselves.

These results, obtained by intentionally broadening the distribution in core block molecular weights in spherical diblock copolymer micelles, provide conclusive support for the single chain exchange dynamics model proposed by Choi et al.<sup>21</sup> Our findings complement the recent study by Zinn et al.<sup>23</sup> on rigorously monodisperse oligomeric diblocks. Whereas the elimination of dispersity drives the relaxation function to an exponential form,  $R(t) \sim K(t, N) = \exp(-t/\tau(N))$ , a bimodal mixture of relatively narrow distribution core blocks greatly expands the spectrum of exchange times, as demonstrated by Figure 4a. These findings suggest that exchange of polymers between micelles can be precisely tailored through blending strategies, including postmixing populations of micelles with different core block molecular distributions.

## AUTHOR INFORMATION

### Corresponding Author

\*E-mail: bates001@umn.edu; lodge@umn.edu.

### Notes

The authors declare no competing financial interest.

## ACKNOWLEDGMENTS

This investigation was supported by Infineum USA L.P. TR-SANS experiments at Oak Ridge National Laboratory's High Flux Isotope Reactor was sponsored by the Scientific User Facilities Division, Office of Basic Energy Sciences, U.S. Department of Energy. We appreciate help with the SANS experiments from Dr. Yuri Melnichenko and Dr. Lilin He.

## REFERENCES

- (1) Kataoka, K.; Harada, A.; Nagasaki, Y. *Adv. Drug Delivery Rev.* **2001**, *47*, 113–131.
- (2) Gaucher, G.; Dufresne, M.; Sant, V. P.; Kang, N.; Maysinger, D.; Leroux, J. J. *Controlled Release* **2005**, *109*, 169–188.
- (3) Declet-Perez, C.; Redline, E. M.; Francis, L. F.; Bates, F. S. *ACS Macro Lett.* **2012**, *1*, 338–342.
- (4) Ruzette, A.; Leibler, L. *Nat. Mater.* **2005**, *4*, 19–31.
- (5) Anderson, W. Block Copolymers as Viscosity Index Improvers for Lubrication Oils. U.S. Patent 3763044, 1973.
- (6) Mandema, W.; Emeis, C. A.; Zeldenrust, H. *Makromol. Chem.* **1979**, *180*, 2163–2174.
- (7) Schouten, M.; Dorrepaal, J.; Stassen, W. J. M.; Vlask, W. A. H. M.; Mortensen, K. *Polymer* **1989**, *30*, 2038–2046.
- (8) Zhulina, E. B.; Adam, M.; LaRue, I.; Sheiko, S. S.; Rubinstein, M. *Macromolecules* **2005**, *38*, 5330–5351.
- (9) Hamley, I. W. *The Physics of Block Copolymers*; Oxford University Press: Oxford; New York, 1998.

- (10) Israelachvili, J. N. *Intermolecular and Surface Forces*, 2 ed.; Academic Press: San Diego, 1991.
- (11) Willner, L.; Poppe, A.; Allgaier, J.; Monkenbusch, M.; Richter, D. *Europhys. Lett.* **2001**, *55*, 667–673.
- (12) Semenov, A. N. *J. Exp. Theor. Phys.* **1985**, *61*, 733.
- (13) Won, Y.; Davis, H. T.; Bates, F. S. *Macromolecules* **2003**, *36*, 953–955.
- (14) Jain, S.; Bates, F. S. *Macromolecules* **2004**, *37*, 1511–1523.
- (15) Meli, L.; Santiago, J. M.; Lodge, T. P. *Macromolecules* **2010**, *43*, 2018–2027.
- (16) Lund, R.; Willner, L.; Stellbrink, J.; Lindner, P.; Richter, D. *Phys. Rev. Lett.* **2006**, *96*.
- (17) Lund, R.; Willner, L.; Richter, D.; Dormidontova, E. E. *Macromolecules* **2006**, *39*, 4566–4575.
- (18) Lund, R.; Willner, L.; Richter, D.; Iatrou, H.; Hadjichristidis, N.; Lindner, P. *J. Appl. Crystallogr.* **2007**, *40*, s327–s331.
- (19) Lund, R.; Willner, L.; Lindner, P.; Richter, D. *Macromolecules* **2009**, *42*, 2686–2695.
- (20) Halperin, A.; Alexander, S. *Macromolecules* **1989**, *22*, 2403–2412.
- (21) Choi, S.; Lodge, T. P.; Bates, F. S. *Phys. Rev. Lett.* **2010**, *104*.
- (22) Choi, S.; Bates, F. S.; Lodge, T. P. *Macromolecules* **2011**, *44*, 3594–3604.
- (23) Zinn, T.; Willner, L.; Lund, R.; Pipich, V.; Richter, D. *Soft Matter* **2012**, *8*, 623.
- (24) Choi, S.; Bates, F. S.; Lodge, T. P. *J. Phys. Chem. B* **2009**, *113*, 13840–13848.
- (25) Lai, C.; Russel, W. B.; Register, R. A. *Macromolecules* **2002**, *35*, 841–849.
- (26) Williams, M. L.; Landel, R. F.; Ferry, J. D. *J. Am. Chem. Soc.* **1955**, *77*, 3701–3707.
- (27) Yokoyama, H.; Kramer, E. J. *Macromolecules* **1998**, *31*, 7871–7876.
- (28) Cavicchi, K. A.; Lodge, T. P. *Macromolecules* **2003**, *36*, 7158–7164.
- (29) Barrat, J.; Fredrickson, G. H. *Macromolecules* **1991**, *24*, 6378–6383.
- (30) Sakurai, S.; Hashimoto, T.; Fetters, L. J. *Macromolecules* **1995**, *28*, 7947–7949.